



Study the Behavior of Microspheres Obtained from Natural Polymer as Drug Carriers

Assmaa Sattar Hamzah*^{ORCID}, Nizar Jawad Hadi^{ORCID}

Department of Polymer and Petrochemical Industries, College of Materials Engineering, University of Babylon, Babylon 51001, Iraq

Corresponding Author Email: mm893505@gmail.com

Copyright: ©2025 The authors. This article is published by IETA and is licensed under the CC BY 4.0 license (<http://creativecommons.org/licenses/by/4.0/>).

<https://doi.org/10.18280/acsm.490108>

ABSTRACT

Received: 8 August 2024

Revised: 15 February 2025

Accepted: 20 February 2025

Available online: 28 February 2025

Keywords:

rheology, sodium alginate, water in oil emulsion, microspheres, drug delivery system

Natural polymers have various advantages, such as being inexpensive, nontoxic, biocompatible, and biodegradable. Due to these numerous benefits, alginate microspheres have garnered significant interest as a novel drug delivery system. This study evaluated the influence of sodium alginate concentration on the properties of alginate microspheres and investigated the relationship between the rheological properties and structural characteristics of microspheres. Alginate microspheres were prepared using a single-step water-in-oil emulsion technique. The emulsion used in this study consisted of an alginate solution as the water phase, sunflower oil as the oil phase, and Span 80 as the surfactant. Aceclofenac was employed as the biomacromolecular drug model. The results showed that as alginate concentration increased, the particle size of the microspheres also increased due to the higher viscosity of the alginate solution. The particle size of the alginate microspheres ranged from 32.062 to 475.164 μm , with a spherical shape at all concentrations. The shear-thinning phenomenon is dominant in all alginate solutions. The Power Law and Hersch Bulkley models provided better fits than the Casson and Bingham models for the curve fitting of alginate at different concentrations. The transmittance spectrum of alginate microspheres did not exhibit an additional peak, according to Fourier transform infrared (FTIR) analysis, which explains that the alginate only acted as a carrier for the drug, delivering it to the target position and then degrading without any chemical reaction occurring. The DSC test showed an increase in the melting point compared to that of the pure drug alone when the drug was loaded into microspheres, indicating that the drug was incorporated into the polymer matrix. An increased melting point occurs because the drug is loaded into the microspheres and confined.

1. INTRODUCTION

One of the most commonly used classes of natural polymers in biological applications is alginate. Alginate is widely used in biomedical applications, including drug delivery systems, due to its numerous benefits, such as availability, nontoxicity, biocompatibility, and biodegradability [1, 2]. Various drugs can be encapsulated in alginate [3]. Microencapsulation involves the isolation and preservation of active principles (such as solids, liquids, or gaseous components) from the surrounding medium inside microscopic-sized (1 to 1000 μm) shells or particles. Polymeric materials are typically used to achieve microencapsulation [4].

The technology used to transport the drug to the targeted body region for release and absorption is known as a drug delivery system [5]. Given their ability to overcome the disadvantages of conventional dosage forms, modified release forms are increasingly replacing traditional dosage forms. One of the key factors in drug delivery systems that can impact patient safety during the application phase is particle size. For example, large particles can obstruct small blood vessels and cause embolism [6]. Because these characteristics regulate

microsphere degradation and the drug release profile, particle size and size distribution are crucial [7].

Despite the extensive use of alginate in biomedical applications such as drug delivery, there is a need to investigate the rheological properties of alginate solutions (viscosity, shear stress, shear rate), which can provide insights into the behavior of alginate solutions during the microsphere preparation process. This study investigated the relationship between the rheological properties and structural characteristics of different microspheres (shape, size, size distribution, surface morphology, drug loading). Drug delivery technologies have come a long way from conventional routes like oral tablets and injections to more advanced, controlled, and targeted drug delivery systems [8]. Novel systems include liposomes, polymeric nanoparticles, dendrimers, implantable devices, and microsphere-based formulations. All of these systems have specific advantages and limitations; for example, liposomes are extremely biocompatible but may be unstable, whereas polymeric nanoparticles allow for fine-tuning of pharmacokinetics but often require elaborate synthesis methods. Notably, alginate microspheres represent a novel class of sustained-release systems due to their simple emulsion

production methods, tunable particle size, high drug-loading efficiency, natural biocompatibility, and biodegradability. The advantages of alginate microspheres, which are cost-effective and perform well as drug delivery systems, present a solution for a number of existing pharmaceutical delivery issues [9-11].

The extrusion [12], spray-drying method [13], and emulsion method [14] are the three basic types of alginate microsphere formulation methods. However, alginate particles with sizes varying from hundreds of micrometers to millimeters can be created using the extrusion approach. The spray-drying procedure requires expensive equipment. Compared to previous methods, the emulsion process has some benefits, including the ability to produce microspheres with particle sizes less than 100 μm and minimal equipment costs [15, 16].

In this study, alginate microspheres with and without aceclofenac were prepared using a single water-oil emulsion process with appropriate stirring boundary conditions. Alginate aqueous solution, sunflower oil, Span (80), and aceclofenac were used as the water, oil surfactant, and drug model, respectively. The influence of alginate concentration on the shape, size, and distribution of microspheres was studied by analyzing their rheological properties and flow behavior. The loading of sodium alginate microspheres with the drug was investigated through FTIR and DSC tests.

2. EXPERIMENTAL PART

2.1 Materials used

Pharmaceutical-grade sodium alginate was obtained from Glenham Life Sciences Technology Co., Ltd. in the United Kingdom, and aceclofenac was purchased from HiMedia Laboratories Pvt. Ltd. in India. Sorbitan monooleate (Span 80), sunflower oil, and n-hexane were purchased from Alpha Chemika Co., Pvt. Ltd. in India, and distilled water was used.

2.2 Preparation and characterization of microspheres

The water-in-oil emulsion method was employed to prepare alginate microspheres, both with and without drug encapsulation. Initially, an alginate solution was prepared. Briefly, sodium alginate was weighed (1%, 2%, and 3% w/v) and then dissolved in 100 ml of distilled water, which was stirred at a speed of 600 rpm at 25 $^{\circ}\text{C}$ for 2 hours. Additionally, 1% Span 80 was also weighed, added to the oil phase, and stirred for 5 minutes. From the prepared solution, 10 ml of alginate solution (1%, 2%, and 3% w/v) was taken and added dropwise using a syringe to 50 ml of the oil phase with magnetic stirring (at 900 rpm and 25 $^{\circ}\text{C}$) for 1 hour. The drug-free alginate microspheres in the oil phase were filtered, repeatedly cleaned with n-hexane, and then dried.

By repeating the same procedure to prepare drug-loaded microspheres, an accurately weighed quantity of aceclofenac was added and uniformly dispersed into the alginate solution. The sodium alginate-to-drug ratio was maintained at 9:1 (w/w).

The morphology of the obtained alginate microspheres was examined under an optical microscope in accordance with ASTM F728-81 [17], and the microspheres were measured at 60X magnification using a device called the 1280XEQ-MM300TUSB. Additionally, the morphology was inspected using atomic force microscopy. Using a cone-plate viscometer in accordance with ASTM D7395 [18], the viscosity, shear

thinning, and thickening behaviors, curve fitting, and flow curves of alginate solutions at 1%, 2%, and 3% w/v were determined. Size and size distribution were analyzed using ImageJ software (version 1.02). Fourier transform infrared (FTIR) spectrometry (Bruker, Germany, Electrochemical Department/University of Babylon) and differential scanning calorimetry (DSC Test) were used to determine the drug loading of sodium alginate microspheres.

3. RESULTS AND DISCUSSIONS

3.1 Morphology results

3.1.1 Optical result

Alginate microspheres (AMs) shape, size, and size distribution are critical factors for patient safety during the application period because these characteristics may affect microsphere degradation, drug release kinetics, and therapeutic effectiveness. The alginate concentration is the most significant factor affecting the shape, particle size, and distribution of alginate microspheres.

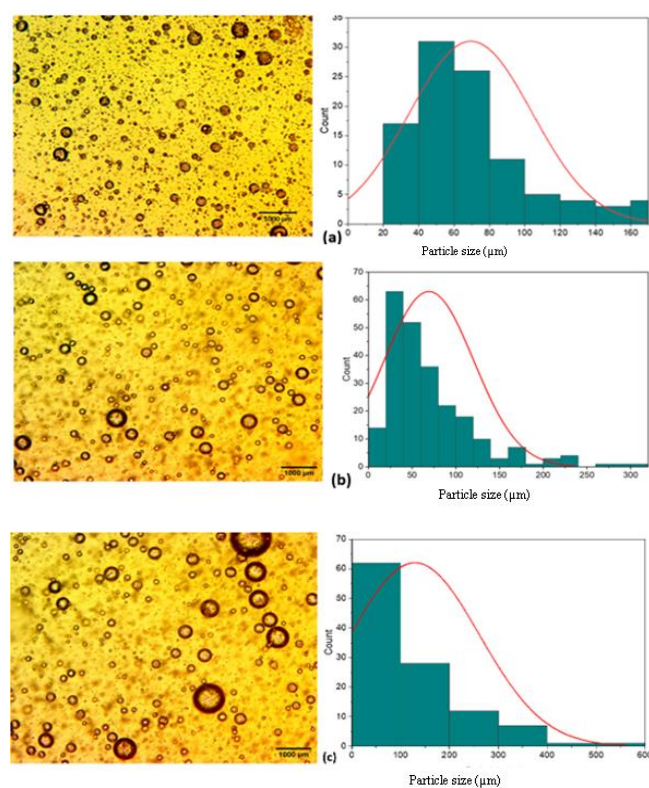


Figure 1. Morphology of microspheres with a)1% b)2% and c) 3% concentration under optical microscope

Figure 1 shows morphology of alginate microspheres at various concentrations. The resulting microspheres were spherical at all concentrations. It was also noted that when the alginate concentration was increased, the particle sizes increased, as shown in Table 1. The interfacial tension between the alginate droplets and the oil phase increased with increasing alginate concentration and viscosity of the alginate solution. Hence, larger microspheres are formed because at high viscosity, this corresponds with the findings of other researchers [19, 20]. The results of the viscosity test showed that the solution viscosity increased from 151.93 cP to 380.64

cP as the alginate concentration increased, as shown in Table 2.

Measurement of the particle size distribution of alginate at various concentrations, using ImageJ software, illustrates how alginate concentration affects the particle size distribution of alginate microspheres (AMs). When the alginate concentrations increase the viscosity increase and lead to the broadening of particle size distribution.

Table 1. Average particles sizes of microspheres

Alginate Concentrations	Average Particle Size (μm)
1%	199.829 \pm 32.062
2%	263.247 \pm 38.012
3%	475.164 \pm 45.212

Table 2. Alginate solutions viscosity

Alginate Concentrations	Viscosity (cP)
1%	151.93
2%	221.73
3%	380.64

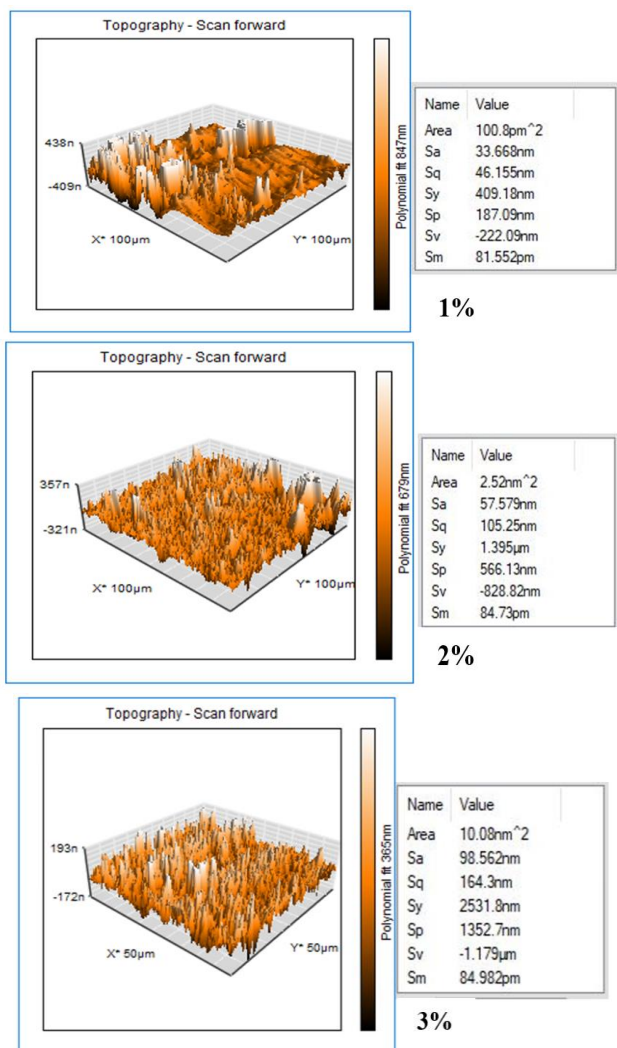


Figure 2. 3D image of alginate microspheres at different concentrations

3.1.2 Atomic force microscopy (AFM) result

AFM provides 3D topographic analysis of the significant differences in the surface roughness of microspheres prepared

using alginate solutions at different concentrations, as shown in Figure 2.

The viscosity of the alginate solution affects the formation and surface properties of the microspheres. The microspheres formed from lower viscosity solutions (1% concentration) exhibited the lowest surface roughness and the smoothest surface topography, with an average roughness (Sa) of 33.668 nm, a root-mean-square roughness (Sq) of 46.155 nm, and a maximum peak-to-valley height (Sv) of -222.09 nm. Lower viscosity allows for a more uniform distribution and smoother surface during formation. Medium viscosity (2% concentration) resulted in moderate surface roughness. The surface was relatively smooth, with an average roughness (Sa) of 45.994 nm, a root-mean-square roughness (Sq) of 60.325 nm, and a maximum peak-to-valley height (Sv) of 275.25 nm. Higher viscosity (3% concentration) produced microspheres with greater surface roughness (Sa and Sq values). The microspheres displayed the most irregular surface, with pronounced peaks and valleys, evidencing the highest surface roughness among the samples, including the highest average roughness (Sa) of 98.562 nm, root-mean-square roughness (Sq) of 164.3 nm, and maximum peak-to-valley height (Sv) of -1,179 nm. This result corresponds to the observation that the alginate solution at 3% concentration exhibits the highest viscosity compared to the other concentrations.

3.2 Rheological results

A cone-plate viscometer was used to evaluate the viscosity of alginate based on the shear rate and concentration. The results were then fitted to fluid models using rheology software. Figures 3 and 4 show the relationship between viscosity and shear rate, as well as shear rate and shear stress of alginate solutions at various concentrations.

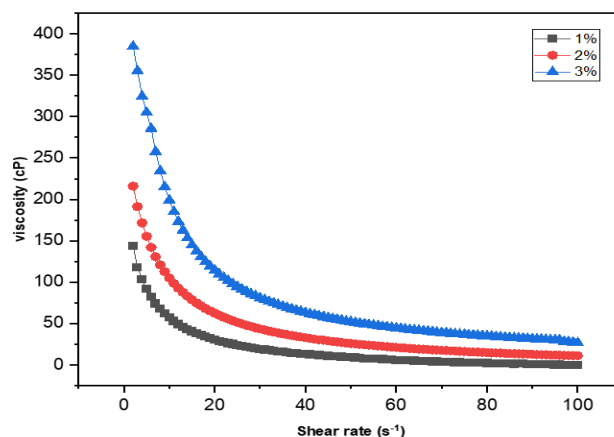


Figure 3. Viscosity curve for alginate solutions

The flow behavior demonstrates non-Newtonian flow (pseudoplastic type). The shear-thinning phenomena dominate in all alginate solutions due to the alignment of the alginate chains caused by the velocity gradient. This finding is crucial because, for instance, the nozzles used in microsphere manufacturing systems can have a small diameter to manage the size of the microspheres and ensure that solutions flow easily. The shear-thinning behavior of the alginate solution facilitates the flow and thereby enhances the emulsion process at low viscosity, leading to the formation of smaller microspheres with a narrow distribution, as shown in the optical and atomic force microscopy results. For this purpose,

the shear stress, shear rate, and shear viscosity are controlled in conjunction with the size and distribution of the microspheres.

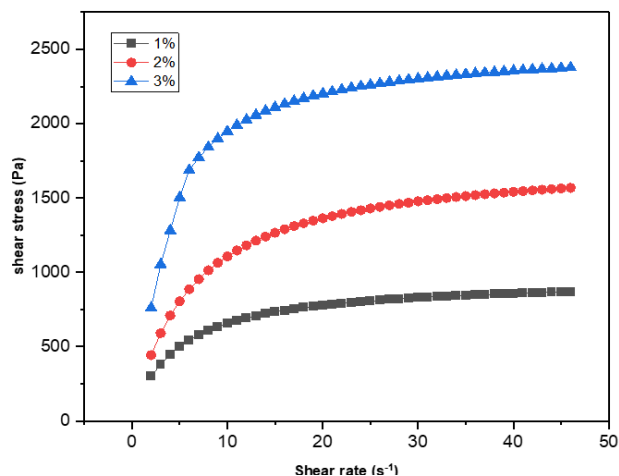


Figure 4. Flow curve for alginate solutions

3.2.1 Mathematical model (Curve fitting)

Curve fitting using non-Newtonian mathematical models for alginate solution flow curves matches experimental rheological data such as viscosity, shear stress, and shear rate with the theoretical models. This process describes the flow behavior under different shear conditions and allows for the accurate characterization of polymer solutions, which is important for optimizing their use in drug delivery systems. Curve fitting helps in the selection of the appropriate concentration and composition of the polymer to achieve the required viscosity and flow behavior. In addition, it prevents sedimentation and phase separation in suspensions and emulsions. The shear stress and viscosity data were measured over a suitable shear rate range using a cone-plate viscometer to capture complete flow behavior. The shear stress-shear rate characteristics were analyzed for all concentrations, as shown in the analysis of the flow curves in Figure 5 and Table 3. The curve fitting software Rheology app program was used to fit the experimental data to the selected models. The proposed program utilizes the Power Law, Herschel-Bulkley, Casson, and Bingham models. The goodness of fit was calculated using statistical R^2 values. A comparison of fits from these models was conducted to determine which best describes the flow curve and rheological behavior.

For the 1% alginate concentration, both the Power Law and Hersch Bulky models showed similar results, with n values of 0.276 and K values of 566.6 and 566.2, respectively, as shown in Table 3 and Figure 5. The R^2 values for these models indicated reasonably good fits, ranging from 0.890539 to 0.896884. The Casson and Bingham models obtained lower R^2 values (0.761398 and 0.60796, respectively).

At the 2% alginate concentration, the Power Law and Hersch Bulky models provided comparable results, with n values of 0.233 and K values of 368.92 and 368.93, respectively. The R^2 values of these models indicated a good fit, ranging from 0.900399 to 0.900536. The Casson and Bingham models obtained lower R^2 values of 0.76895 and 0.612902, respectively.

Finally, at the 3% alginate concentration, the Power Law and Hersch Bulky models exhibited similar n values (0.202) and K values of 1146.2. The R^2 values for these models differed slightly, ranging from 0.745173 to 0.759359. The

Casson and Bingham models obtained lower R^2 values of 0.554674 and 0.345626, respectively. Overall, the Power Law and Hersch Bulky models provided better fits than the Casson and Bingham models for the curve fitting of alginate at different concentrations.

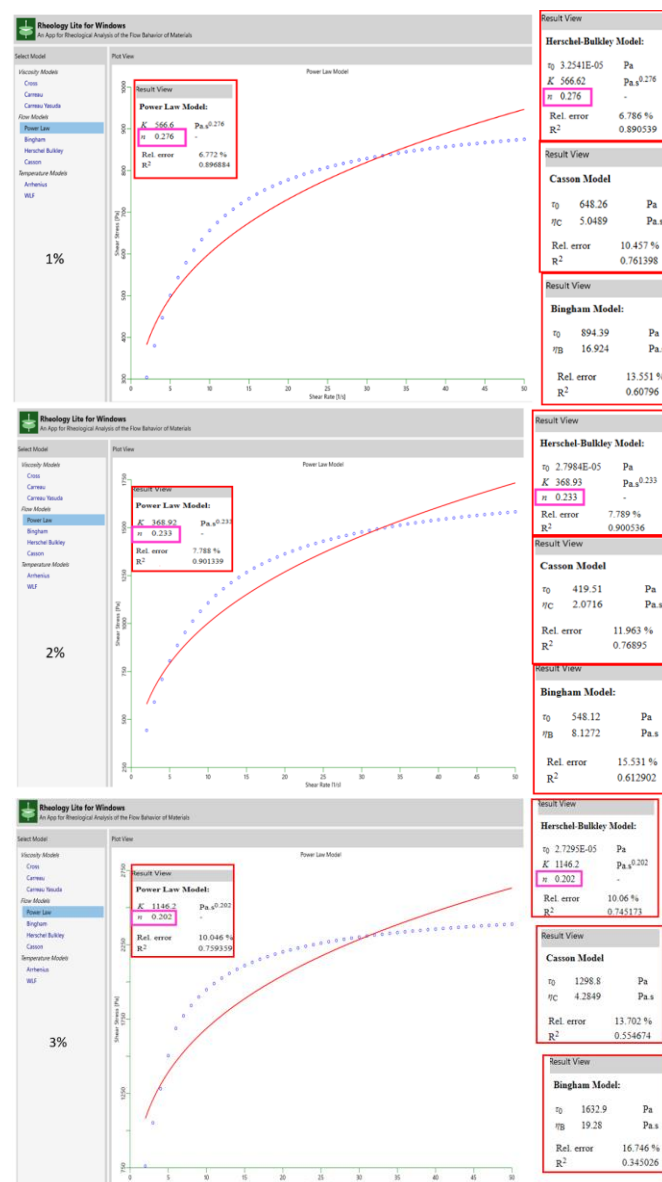


Figure 5. Models' analysis by using Rheology App. for different alginate concentrations

3.3 FTIR result

Fourier transform infrared (FTIR) spectroscopy was used to investigate the loading of the microspheres with the active ingredient, aceclofenac. From the FTIR tests, the typical distinctive bands for a significant functional group of the empty, pure-drug-loaded, and drug-loaded microspheres can be identified (Figure 6). The FTIR results shown in Table 4 provide clear evidence that the drug aceclofenac was effectively loaded into all types of prepared microspheres. A comparison of the FTIR spectra of the individual components, i.e., (a) the microspheres and (b) the active ingredient aceclofenac, with the loaded microspheres (c) shows that the characteristic peaks of aceclofenac did not change after successful encapsulation in the microspheres. The distinct peaks corresponding to aceclofenac included the O-H

stretching at around 3470-3480 cm^{-1} , C-H stretching in the range of 2924-2940 cm^{-1} , C=O stretching between 1728-1744 cm^{-1} , and C-H bending around 1442-1458 cm^{-1} . The presence of these characteristic peaks confirmed the successful incorporation of aceclofenac into the microspheres, confirming the absence of any chemical interactions between

the polymers and the drug. This indicates that the drug is physically entrapped in the polymer structure, which is supported by the absence of new peaks in the spectrum of the drug-loaded microspheres. This result agrees with researchers [21-23].

Table 3. Rheological Model comparison for alginate solutions

Alginate Solutions (wt.%)	Power Law Model	Hersch Bulky Model	Casson Model	Bingham Model
1%	$n = 0.276$	$n = 0.276$		
	$K = 566.6$	$K = 566.2$	Rel.error = 10.457%	Rel.error = 13.551%
	Rel.error = 6.772 % $R^2 = 0.896884$	Rel.error = 6.786 % $R^2 = 0.890539$	$R^2 = 0.761398$	$R^2 = 0.60796$
2%	$n = 0.233$	$n = 0.233$		
	$K = 368.92$	$K = 368.93$	Rel.error = 11.963%	Rel.error = 15.531%
	Rel.error = 7.788 % $R^2 = 0.900399$	Rel.error = 7.789 % $R^2 = 0.900536$	$R^2 = 0.76895$	$R^2 = 0.612902$
3%	$n = 0.202$	$n = 0.202$		
	$K = 1146.2$	$K = 1146.2$	Rel.error = 13.702%	Rel.error = 16.746 %
	Rel.error = 10.046 % $R^2 = 0.759359$	Rel.error = 10.06 % $R^2 = 0.745173$	$R^2 = 0.554674$	$R^2 = 0.345626$

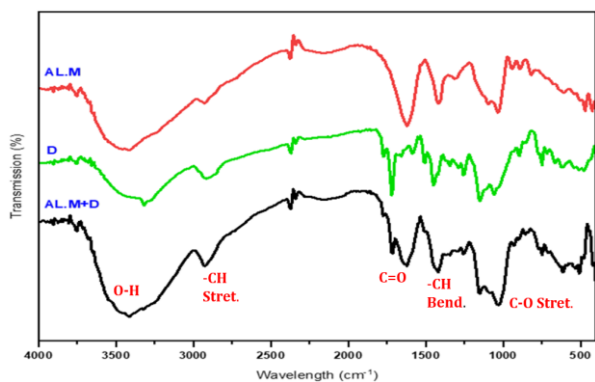


Figure 6. FTIR spectrum for: (a) alginate microspheres (b) aceclofenac drug (c) Microspheres loaded by aceclofenac

Table 4. Characteristic peaks value of FTIR spectra of alginate microspheres loading drug

Wavenumber (cm^{-1})	Functional Group	Mode of Vibration
Aceclofenac		
3317.56	O-H	stretching
2916.37	C-H	stretching
1771.35	C=O	stretching
1450.47	C-H	bending
1149.57	C-O	stretching
Alginate microspheres		
3417.86	O-H	stretching
2931.80	C-H	stretching
1620.21	C=O	stretching
1419.61	C-H	bending
1033.85	C-O	stretching
Alginate microsphere + aceclofenac drug		
3479.58	O-H	stretching
2939.52	C-H	stretching
1728.22	C=O	stretching
1442.75	C-H	bending
1157.29	C-O	stretching

3.4 DSC results

DSC was performed to characterize and study the thermal behaviors of aceclofenac, both as a standalone drug and when

loaded into microspheres. The DSC curve of aceclofenac is shown in Figure 7; it indicates its crystalline nature by exhibiting a single, sharp endothermic peak corresponding to the melting point of the drug. The endothermic peak in the DSC curve represents the energy absorbed during melting as the drug transitions from a solid to a liquid state. The measured melting point of the drug was found to be 149.42°C, which is well within the range reported in the literature specification of 149-150°C, confirming the identity and purity of the aceclofenac powder.

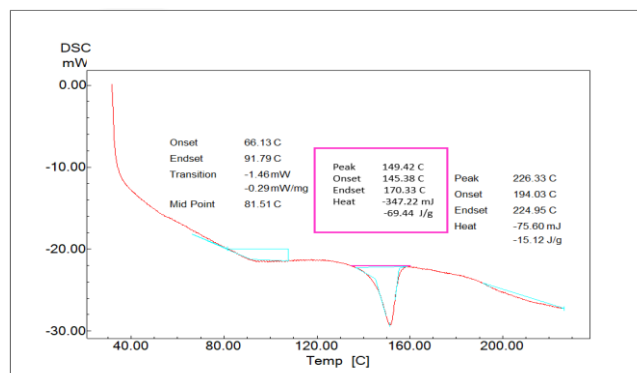


Figure 7. DSC thermogram of pure aceclofenac drug

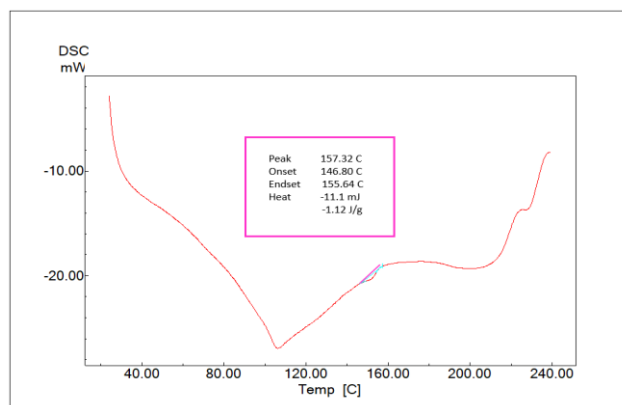


Figure 8. DSC thermogram of alginate microspheres loading drug

It can be recognized that the DSC curve, as shown in Figure 8, when aceclofenac was loaded into the microspheres, showed different thermal behavior compared to the pure drug. Instead of a sharp melting endotherm, the microsphere formulation exhibited a broad, less distinct thermal transition. This change in the thermal properties of the drug indicates that the encapsulation process has resulted in the drug being uniformly dispersed in the polymer matrix at the molecular level, which may also be attributed to the fact that the drug is no longer in its pure crystalline form. It may be present in an amorphous or partially amorphous state within the polymer matrix.

This change in the physical state of the drug indicates physical interactions and disruption of the crystalline structure rather than the formation of new chemical compounds. The FTIR data support this interpretation by confirming the absence of new chemical bonds or interactions between the drug and polymer. The absence of new FTIR peaks confirms that the changes observed in the DSC curve are primarily physical, with no significant chemical reactions having taken place. This was also confirmed by the FTIR results.

The DSC test showed an increase in the melting point compared to that of the pure drug alone when the drug was loaded into microspheres, indicating that the drug was incorporated into the polymer matrix. The increased melting point occurs because the drug is loaded into the microspheres and confined within the polymer matrix. The drug molecules are dispersed or encapsulated within the microsphere structure, surrounded by the polymer material. This confinement restricts the molecular motion of the drug molecules, trapping them within the polymer matrix and preventing them from moving freely or undergoing the phase transition associated with melting. The confinement effect increases the energy barrier for the drug molecules to transition from the solid to the liquid state. As a result, the drug molecules require higher temperatures to overcome confinement and reach their melting point. This resulted in an increased melting temperature (T_m) in the drug-loaded microspheres compared with that of the pure drug. The confinement effect can be attributed to the physical properties of the polymer matrix, such as its rigidity and density.

Differential scanning calorimetry (DSC) analysis demonstrated the thermal transitions that occurred during the drug encapsulation in a quantitative manner. The DSC curve of pure aceclofenac showed a sharp endothermic peak at a melting temperature (T_m) of 149.42°C, and an enthalpy change (ΔH) of 69.44 J/g, which was in agreement with its crystalline state. In comparison, the drug-encapsulated alginate microspheres exhibited a temperature transition that was both shifted and broadened (with a higher T_m of 157.32°C) and a greatly reduced ΔH of 1.12 J/g. These differences, based on quantitative analysis, indicate that aceclofenac incorporated in the microspheres is in a molecular state dispersed within the polymer matrix, which significantly modifies the energetic barrier to melting compared to the as-received aceclofenac, due to the confinement effects related to the alginate microspheres.

4. CONCLUSIONS

The results of this study indicate that the concentration of the alginate solution strongly influences the shape, size, and distribution of alginate microspheres. A water-oil emulsion

technique proved to be an effective, low-cost process for producing both drug-free and drug-loaded spherical alginate microspheres. Alginate microspheres ranged in size from 32.062 to 475.164 μm . As the viscosity of the alginate solution increased with higher alginate concentration, the size of the microspheres also increased. The optimal alginate concentration was 1% w/v. At that concentration, the microspheres exhibited a narrow distribution and an average particle size of $199.829 \pm 32.062 \mu\text{m}$, making them suitable for use in drug delivery systems. Morphological results indicate that the microspheres were spherical with moderately rough surfaces. The results also show that shear stress, shear rate, and shear viscosity clearly control the size and distribution of the microspheres. The Power Law and Herschel-Bulkley models provided better fits than the Casson and Bingham models for the curve fitting of alginate at different concentrations. FTIR and DSC analyses confirmed the loading of aceclofenac within the microspheres, with no indication of chemical bonding between the drug and the polymer. The drug was physically trapped within the polymer structure, as evidenced by the absence of new peaks. The results of this study highlight the potential for using alginate in controlled drug delivery systems. Future research could focus on further investigations into the rheological properties of alginate solutions under different conditions, such as temperature and pH. In addition, in vivo studies should be conducted to verify the effectiveness of alginate-based drug delivery systems.

REFERENCES

- [1] Wang, J., Liu, S., Huang, J., Ren, K., Zhu, Y., Yang, S. (2023). Alginate: Microbial production, functionalization, and biomedical applications. *International Journal of Biological Macromolecules*, 242: 125048. <https://doi.org/10.1016/j.ijbiomac.2023.125048>
- [2] Li, Q.Q., Xu, D., Dong, Q.W., Song, X.J., Chen, Y.B., Cui, Y.L. (2024). Biomedical potentials of alginate via physical, chemical, and biological modifications. *International Journal of Biological Macromolecules*, 134409. <https://doi.org/10.1016/j.ijbiomac.2024.134409>
- [3] Morparia, S., Suvana, V. (2024). Recent advancements in applications of alginates in drug delivery, tissue engineering, and biomedical field. *The Natural Products Journal*, 14(9): 83-100. <https://doi.org/10.2174/0122103155284365240103063024>
- [4] Yan, C., Kim, S.R. (2024). Microencapsulation for pharmaceutical applications: A review. *ACS Applied Bio Materials*, 7(2): 692-710. <https://doi.org/10.1021/acsabm.3c00776>
- [5] Kumar, M., Mandal, U.K., Mahmood, S. (2023). Novel drug delivery system. In *Advanced and Modern Approaches for Drug Delivery*, pp. 1-32. <https://doi.org/10.1016/B978-0-323-91668-4.00012-5>
- [6] Khan, S.A., Ali, H. (2022). Novel drug delivery systems. In *Essentials of Industrial Pharmacy* (pp. 235-250). https://link.springer.com/chapter/10.1007/978-3-030-84977-1_14
- [7] Deng, J., Ye, Z., Zheng, W., Chen, J., Gao, H., Wu, Z., Chan, G., Wang, Y., Cao, D., Wang, Y., Lee, S.M.Y., Ouyang, D. (2023). Machine learning in accelerating microsphere formulation development. *Drug Delivery*

- and Translational Research, 13(4): 966-982. <https://doi.org/10.1007/s13346-022-01253-z>
- [8] Ezike, T.C., Okpala, U.S., Onoja, U.L., Nwike, C.P., Ezeako, E.C., Okpara, O.J., Okoroafor, C.C., Eze, S.C., Kalu, O.L., Odoh, E.C., Nwadike, U.G., Ogbodo, J.O., Umeh, B.U., Ossai, E.C., Nwanguma, B.C. (2023). Advances in drug delivery systems, challenges and future directions. *Heliyon*, 9(6): e17488. <https://doi.org/10.1016/j.heliyon.2023.e17488>
- [9] Yu, L., Liu, S., Jia, S., Xu, F. (2023). Emerging frontiers in drug delivery with special focus on novel techniques for targeted therapies. *Biomedicine & Pharmacotherapy*, 165: 115049. <https://doi.org/10.1016/j.biopha.2023.115049>
- [10] Yang, C., Zhang, Z., Gan, L., Zhang, L., Yang, L., Wu, P. (2023). Application of biomedical microspheres in wound healing. *International Journal of Molecular Sciences*, 24(8): 7319. <https://doi.org/10.3390/ijms24087319>
- [11] Li, Q., Chang, B., Dong, H., Liu, X. (2023). Functional microspheres for tissue regeneration. *Bioactive Materials*, 25: 485-499. <https://doi.org/10.1016/j.bioactmat.2022.07.025>
- [12] Li, X., Li, L., Wang, D., Zhang, J., Yi, K., Su, Y., Luo, J., Deng, X., Deng, F. (2024). Fabrication of polymeric microspheres for biomedical applications. *Materials Horizons*, 11(12): 2820-2855. <https://doi.org/10.1039/D3MH01641B>
- [13] Berraquero-García, C., Pérez-Gálvez, R., Espejo-Carpio, F.J., Guadix, A., Guadix, E.M., García-Moreno, P.J. (2023). Encapsulation of bioactive peptides by spray-drying and electrospraying. *Foods*, 12(10): 2005. <https://doi.org/10.3390/foods12102005>
- [14] Zhang, Z., He, X., Zeng, C., Li, Q., Xia, H. (2024). Preparation of cassava starch-gelatin yolk-shell microspheres by water-in-water emulsion method. *Carbohydrate Polymers*, 323: 121461. <https://doi.org/10.1016/j.carbpol.2023.121461>
- [15] Ruan, L., Su, M., Qin, X., Ruan, Q., Lang, W., Wu, M., Chen, Y., Lv, Q. (2022). Progress in the application of sustained-release drug microspheres in tissue engineering. *Materials Today Bio*, 16: 100394. <https://doi.org/10.1016/j.mtbio.2022.100394>
- [16] Jurić, S., Šegota, S., Vinceković, M. (2019). Influence of surface morphology and structure of alginate microparticles on the bioactive agents release behavior. *Carbohydrate Polymers*, 218: 234-242. <https://doi.org/10.1016/j.carbpol.2019.04.096>
- [17] Echlin, P. (2011). *Handbook of sample preparation for scanning electron microscopy and X-ray microanalysis*. Springer Science & Business Media.
- [18] Gosselin, C.A. (2024). ASTM standards for measuring viscosity. *CoatingsTech*, 21(3): 63.
- [19] Uyen, N.T.T., Hamid, Z.A., Nurazreena, A. (2019). Fabrication and characterization of alginate microspheres. *Materials Today: Proceedings*, 17: 792-797. <https://doi.org/10.1016/j.matpr.2019.06.364>
- [20] Fernando, I.P.S., Kirindage, K.G.I.S., Jeon, H.N., Han, E.J., Jayasinghe, A.M.K., Ahn, G. (2022). Preparation of microspheres by alginate purified from *Sargassum horneri* and study of pH-responsive behavior and drug release. *International Journal of Biological Macromolecules*, 202: 681-690.
- [21] Ashok, P., Tyagi, Y., Parveen, M.H., Kumar, V. (2024). Formulation and evaluation of sustained release microspheres resin loaded aceclofenac. *World Journal of Pharmaceutical Research*, 13(5): 892-903.
- [22] Mollah, M.Z., Faruque, M.R., Bradley, D.A., Khandaker, M.U., Al Assaf, S. (2023). FTIR and rheology study of alginate samples: Effect of radiation. *Radiation Physics and Chemistry*, 202: 110500. <https://doi.org/10.1016/j.radphyschem.2022.110500>
- [23] Andiran, V., Kannan, K. (2023). Design and evaluation of controlled onset extended-release system for chronotherapeutic delivery of aceclofenac. *Research Journal of Pharmacy and Technology*, 16(3): 1041-1046. <http://doi.org/10.52711/0974-360X.2023.00174>